UNSTRUCTURED GRIDS AND AN ELEMENT BASED CONSERVATIVE APPROACH FOR COMPOSITIONAL RESERVOIR SIMULATION

Francisco Marcondes, marcondes@ufc.br
Federal University of Ceará – Centro de Tecnologia - Campus do Pici – Bloco 714 – 60455-760 Fortaleza- CE –Brazil

Kamy Sepehrnoori, kamys@mail.utexas.edu
The University of Texas at Austin - Petroleum and Geosystems Engineering - 1 University Station C0300 - Austin, TX - USA 78712-0228

Abstract. *This paper presents an investigation of an element-based approach for a compositional reservoir simulator using unstructured grids. In this approach, the reservoir is discretized using a mixed two-dimensional mesh using quadrilateral and triangle elements. Thus, complex boundaries and geologic faults of a reservoir can easily be modeled. After the initial step of discretization, each element is divided into sub-elements and the mass balance for each component is developed for each sub-element. The equations for each control-volume using a cell vertex construction are formulated through the contribution of different neighbored elements. The results using the method presented above in conjunction with a compositional reservoir simulation case study are presented, as well as a comparison with a commercial reserservoir simulator that uses a similar approach with triangular elements.*

Keywords*: compositional model, unstructured grids, petroleum reservoir simulation*

1. INTRODUCTION

Unstructured meshes present an important step in the complete reservoir discretization, since there is no line or surface restriction similar to that found in structured meshes. Unstructured meshes have been used for a long time in petroleum reservoir simulation, (Forsyth, 1990; Fung *et al.*, 1991; Gottardi and Dall'Ollio, 1992; Verma and Aziz, 1997). The methodology used by the previous authors in petroleum reservoir simulation and computational fluid dynamics literature is called Control Volume Based Finite Element Method (CVFEM). In most approaches in petroleum reservoir simulation, the approximate equations for multiphase fluid flow are obtained from the single phase flow and then the transmissibilities are multiplied by the mobilities and densities in order to obtain the equations for the multiphase flow. Using ideas from Raw (1985) and Baliga and Patankar (1983), in conjunction with quadrilateral and triangles, respectively, Cordazzo (2004) and Cordazzo *et al.* (2004a-b) have used a similar approach to CVFEM to simulate a water flooding case study, but the approximate equations were obtained using the multiphase approach. These authors demonstrated that the equations obtained from a single phase flow equation do not correctly approximate the equations for multiphase flow. If this approach is used, the angles of meshes must be right angles or smaller, in order to avoid negative transmissibilities. This restriction can be difficult to follow for most reservoirs, due mainly to the heterogeneity of the medium, fractures, faults, or even generic boundaries of the reservoirs. These authors called their methodology Element Based Finite Volume method (EbFVM). We also believe that such an approach is more suitable than CFVEM for discretization of the domain of interest, since, as explained by Maliska (2004), we have a methodology that still follows the conservative principles at the discrete level and only borrows the idea of elements and shape functions from the finite element method. Cordazzo (2004) used an IMPES (Implicit Pressure Explicit Saturation) formulation in conjunction with very distorted triangular and quadrilateral elements with EbFVM to simulate a two phase fluid flow (oil and water) problem. Excellent results were obtained with very little grid orientation.

Although compositional reservoir simulations play an important role in oil recovery processes, to the best of our knowledge, EbFVM has not been applied for simulating compositional, multiphase, multi-component fluid-flow problems. This work presents the implementation of a hybrid EbFVM in conjunction with quadrilateral and triangular elements in an in-house compositional simulator called GPAS (General Purpose Adaptive Simulator). GPAS was developed at the Center for Petroleum and Geosystems Engineering at the University of Texas at Austin for the simulation of enhanced recovery processes. GPAS is a fully implicit, multiphase/multi-component simulator which can handle the simulation of several enhanced oil recovery processes. This simulator is divided into two main modules: Framework and EOScomp. Framework is responsible for input/output and memory allocation, while EOScomp handles the computations for flash calculation and solution of non-linear equations arising from the discretization of the governing equations. Details of EOScomp and Framework modules can be found in Wang *et al.* (1997) and Parashar *et al.* (1997), respectively.

2. PHYSICAL MODEL

Isothermal, multi-component, multiphase fluid flow in a porous medium can be described using three types of equations: the component-material balance equation, phase equilibrium equation, and equation for constraining phase saturations and component concentrations (Wang *et al.*, 1997).

The material balance equation for the i-th component for a full symmetric permeability tensor using the Einstein notation can be written as

$$\frac{\partial(\phi N_i)}{\partial t} - \nabla\bullet\left[\sum_{j=1}^{n_p}\xi_j\, x_{ij}\,\lambda_j \overline{\overline{K}}\bullet\nabla\Phi_j\right] - \frac{q_i}{V_b} = 0\ ;\ i=1,2,..,n_c \tag{1}$$

In Equation (1), n_c is the number of hydrocarbon components, n_p is the number of phases present in the reservoir, ϕ is the porosity, N_i is the moles of the i-th component per unit of pore volume, ξ_j and λ_j are the molar density and relative mobility of the j-th phase respectively, x_{ij} is the molar fraction of the i-th component in the j-th phase, $\overline{\overline{K}}$ is the absolute permeability tensor, and V_b is the volume of control-volume that has a well. Φ_j is the potential of the j-th phase and is given by

$$\Phi_j = P_j - \gamma_j Z \tag{2}$$

Where P_j denotes the pressure of the j-th phase and Z is depth, which is positive in a downward direction.

The first partial derivative of the total Gibbs free energy with respect to the independent variables gives the equality of component fugacities among all phases,

$$f_i = f_i^{\,j} - f_i^{\,r} = 0\ \ ;\ \ i=1,....,n_c\quad ;\quad j=2,.....,n_p \tag{3}$$

In Equation (3), $f_i^{\,j} = \ln\left(x_{ij}\,\phi_{ij}\right)$, where ϕ_{ij} is the fugacity coefficient of component i in the j-th phase, r denotes the reference phase, and n_c is the number of components excluding the water. The restriction of the molar fraction is used to obtain the solution of Eq. (3),

$$\sum_{i=1}^{n_c} x_{ij} - 1 = 0\ ,\ j=2,..,n_p\quad ;\quad \sum_{i=1}^{n_c}\frac{z_i(K_i-1)}{1+\nu(K_i-1)} = 0 \tag{4}$$

where z_i is the overall molar fraction of the i-th component, K_i is the equilibrium ratio for the i-th component, and ν is the mole fraction of the gas phase in the absence of water. The closure equation comes from the volume constraint, i.e, the available pore volume of each cell must be filled by all phases present in the reservoir. This constraint gives rise to the following equation:

$$V_b\sum_{i=1}^{n_c+1}(\phi N_i)\sum_{j=1}^{n_p} L_j\,\bar{v}_j - V_p = 0 \tag{5}$$

where V_b is the bulk volume, V_p is the pore volume, and $\bar{v}_j$ is the molar volume of the j-th phase. In GPAS the unknown primary variables are water pressure P_w, $N_1,..,N_{nc}$, $\ln K_1,..,\ln K_{nc.}$

3. APPROXIMATE EQUATION

In the EbFVM, each element is divided into sub-elements which will be referred to as sub-control volumes. The conservation equations (Eq. (1)) need to be integrated in these sub-control volumes. Figure 1 presents a triangular and quadrilateral element and all of the sub-control volumes associated with each element. Integrating Equation (1) for each of the sub-control volumes and in time, and applying the Gauss theorem for the advective term we obtain

$$\int_V \frac{\partial(\phi N_i)}{\partial t}dV - \int_A\sum_{j=1}^{n_p}\xi_j\, x_{ij}\,\lambda_j\overline{\overline{K}}\bullet\nabla\Phi_j\bullet\overrightarrow{dA} - \int_V\frac{q_i}{V_b} = 0\ ;\ i=1,2,..,n_c \tag{6}$$

To evaluate the first and second terms of Eq. (6), it is necessary to define the shape functions. For triangles and quadrilaterals, linear and bi-linear shape functions as defined through Eqs. (7) and (8), will be used, respectively.

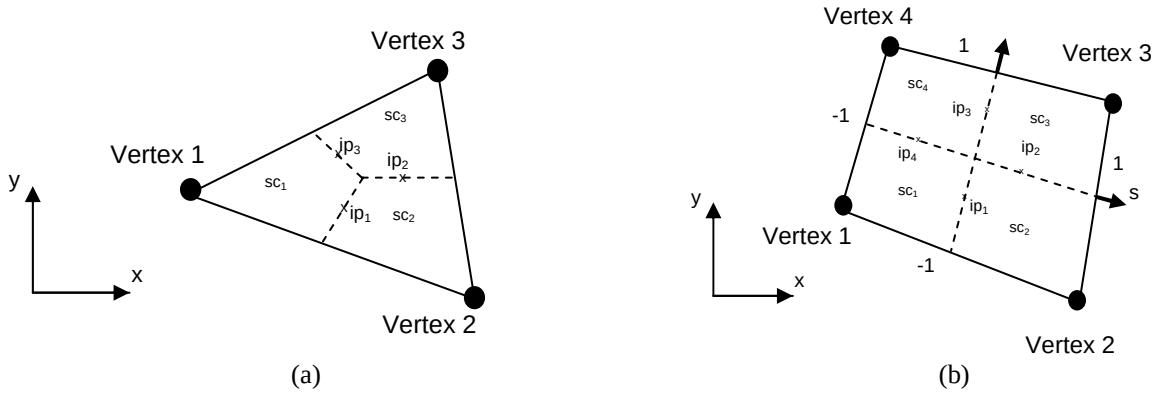

(a) (b)

Figure 1. Triangle and quadrilateral elements and their respective sub-control volumes

$$N_1(s,t)=1-s-t \;\; ; \;\; N_2(s,t)=s \;\; ; \;\; N_3(s,t)=t \tag{7}$$

$$\begin{aligned} &N_1(s,t)=\frac{1}{4}(1+s)(1+t) \;\; ; \;\; N_2(s,t)=\frac{1}{4}(1-s)(1+t) \;\; ; \\ &N_3(s,t)=\frac{1}{4}(1-s)(1-t) \;\; ; \;\; N_4(s,t)=\frac{1}{4}(1+s)(1-t) \end{aligned} \tag{8}$$

Using the shape functions any physical properties or positions can be evaluated inside an element as

$$x(s,t)=\sum_{i=1}^{Nv} N_i\, x_i \;\; ; \;\; y(s,t)=\sum_{i=1}^{Nv} N_i\, y_i \;\; ; \;\; \Phi_j(s,t)=\sum_{i=1}^{Nv} N_i\, \Phi_{ji} \tag{9}$$

where N_v denotes the number of vertex for each element. Elements using the same shape function for coordinates and physical properties are known as isoparametric elements (Hughes, 1987). Using the shape functions, gradients of potentials can be easily evaluated as

$$\frac{\partial \Phi_j}{\partial x}=\sum_{i=1}^{Nv}\frac{\partial N_i}{\partial x}\Phi_{ji} \;\; ; \;\; \frac{\partial \Phi_j}{\partial y}=\sum_{i=1}^{Nv}\frac{\partial N_i}{\partial y}\Phi_{ji} \tag{10}$$

To evaluate the gradients, it is necessary to obtain the derivatives of shape functions relative to x and y. These derivatives are given by

$$\frac{\partial N_i}{\partial x}=\frac{1}{\det(J_t)}\left(\frac{\partial N_i}{\partial s}\frac{\partial y}{\partial t}-\frac{\partial N_i}{\partial t}\frac{\partial y}{\partial s}\right) \;\; ; \;\; \frac{\partial N_i}{\partial y}=\frac{1}{\det(J_t)}\left(\frac{\partial N_i}{\partial t}\frac{\partial x}{\partial s}-\frac{\partial N_i}{\partial s}\frac{\partial x}{\partial t}\right) \tag{11}$$

where J_t is the Jacobian of the transformation and it is given by

$$\det(J_t)=\left(\frac{\partial x}{\partial s}\frac{\partial y}{\partial t}-\frac{\partial x}{\partial t}\frac{\partial y}{\partial s}\right) \tag{12}$$

Further details of the expressions given by Eq. (11) can be found in Maliska (2004) and Cordazzo (2004). To perform the integral of Eq. (6), it is necessary to define the volumes of each sub-control volume and the area of each interface. The volumes of each sub-control for triangles and quadrilaterals, respectively, are given by

$$Vscv_i=\frac{\det(J_t)\,\Delta s\,\Delta t\,h}{6} \tag{13}$$

$$Vscv_i=\det(J_t)\,\Delta s\,\Delta t\,h \tag{14}$$

where h is the thickness of the reservoir. For quadrilateral det(J_t) needs to be evaluated at the center of each sub-control volume. The area of each interface, reading a counterclockwise, is given by

$$\overrightarrow{dA} = h\,dy\,\vec{i} - h\,dx\,\vec{j} \tag{15}$$

Substituting Eqs. (13) and (14) for the accumulation term, and (15) for the advective flux into Eq. (6), and evaluating the fluid properties through a fully implicit procedure the following equations for the two mentioned terms are obtained:

$$Acc_{m,i} = Vscv_{m,i}\left(\left(\frac{\phi N_m}{\Delta t}\right)_i - \left(\frac{\phi N_m}{\Delta t}\right)_i^o\right) \quad ; \quad m = 1, N_v \tag{16}$$

$$F_{m,i} = \int_A \sum_{j=1}^{np} \xi_j\, x_{ij}\, \lambda_j \overline{\overline{K}} \bullet \nabla\Phi_j \bullet \overrightarrow{dA} = \int_A \sum_{j=1}^{np} \xi_j\, x_{ij}\, \lambda_j K_{np} \frac{\partial \Phi_j}{\partial x_p} dA_n \quad ; \quad m = 1, N_v \; ; \; n, p = 1, 2 \tag{17}$$

By inspecting Eq. (17), it can be inferred that it is necessary to evaluate molar densities, molar fraction and mobilities in two interfaces of each sub-control volume. To evaluate these properties, an upwind scheme based on the ideas of Cordazzo *et al*. (2004) will be used. The mobilities and other fluid properties are evaluated at the integration point 1 of Fig. 1a, for instance, by

$$\begin{aligned} &\lambda_{j1} = \lambda_{j2} \quad if \quad \overline{\overline{K}}.\nabla\Phi_j.\overrightarrow{dA}\Big|_{ip1} \le 0 \\ &\lambda_{j1} = \lambda_{j1} \quad if \quad \overline{\overline{K}}.\nabla\Phi_j.\overrightarrow{dA}\Big|_{ip1} > 0 \end{aligned} \tag{18}$$

Inserting Eqs. (16) and (17) into Eq. (6), the following equation for each element is obtained:

$$Acc_{m,i} + F_{m,i} + q_i = 0 \quad ; \quad m = 1, N_v \; ; \; i = 1, Nc+1 \tag{19}$$

Equation (19) denotes the conservation for each sub-control volume of each element. Now, it is necessary to assemble the equation of each control volume obtaining the contribution of each sub-control volume that shares the same vertex. This process is like the assembling of the stiffness global matrix in the finite element method. Figure 2 presents a control-volume around vertex 5 (dark continuous lines) that will receive contributions from sc1 of element 1, sc3 of element 2, sc4 of element 6, and sc1 of element 7.

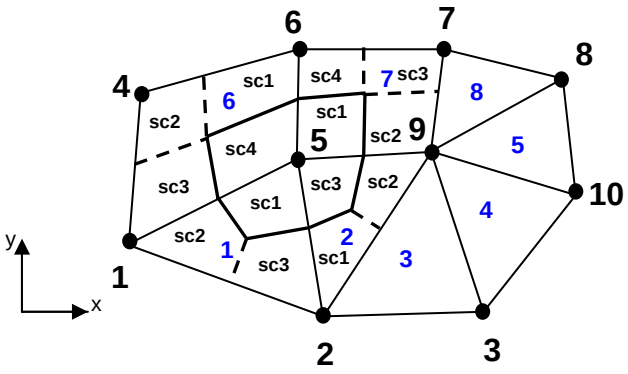

Figure 2. Control volume

4. TEST PROBLEMS

In order to present the application of EbFVM, three simulation case studies were carried out. Case 1 is the simulation of water flooding in a quarter-of-five spot with the simultaneous flow of water and oil. The results for this case will be compared to the results using a commercial simulator, which uses a black-oil model. Also, only triangular

meshes will be used since the commercial simulator has the CVFEM formulation with only triangle elements. Figure 3 presents one of the grid configuration used for this study. Table 1 presents the fluid and physical properties. The relative permeability curves for this case are shown in Fig. 5b.

Table 1. Input data for Case 1.

Reservoir data	Initial conditions	Physical properties and well conditions
Reservoir dimension ($L_x = L_y$ = 170.69 m, L_z = 3.048 m) Absolute permeability ($K_{xx} = K_{yy} = K_{zz}$) = 1.0×10^{-13} m^2 (100 mD) Porosity = 0.20	Water saturation S_{wi} = 0.2 Reservoir pressure = 3.45 MPa (500 psi) Overall fraction of hydrocarbon components (C10) = 1.0	Water viscosity = 1×10^{-3} Pa.s Water injection rate = 2.208×10^{-4} m^3/s (50 barrels/d) Bottom hole pressure = 2.07 MPa (300 psi)

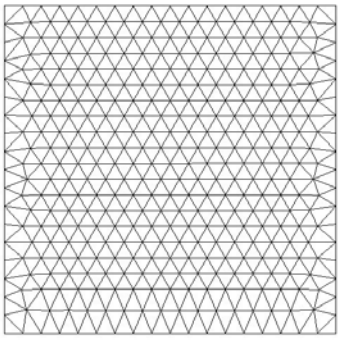

Figure 3. A 695 elements and 385 nodes triangular mesh used for case 1

The second case presents the simulation of a quarter-of-five spot pattern, but now we have gas injection and the reservoir contains oil that has been characterized using three hydrocarbon components. For this case, we have tested meshes with quadrilaterals, triangles, and hybrid with triangles around the wells and quadrilaterals in the rest of reservoir. Figure 4 shows the hybrid mesh employed to this case. The fluid and physical properties are shown in Tab. 2, and relative permeability curves are given in Fig. 5.

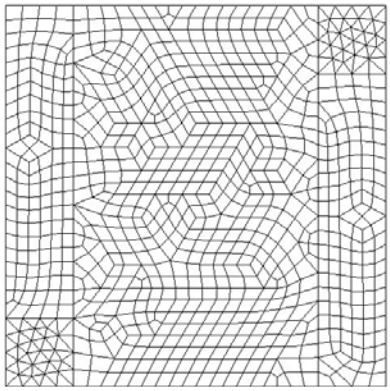

Figure 4. A 918 elements and 921 nodes hybrid mesh used for case 2

Table 2. Input data for Case 2.

Reservoir data	Initial conditions	Physical properties and well conditions
Reservoir dimension ($L_x = L_y$ = 170.69 m, L_z = 30.48 m) Absolute permeability ($K_{xx} = K_{yy} = K_{zz}$) = 1.0×10^{-14} m^2 (10mD) Porosity = 0.350	Water saturation S_{wi} = 0.17 Reservoir pressure = 10.35 MPa (1500 psi) Overall fraction of hydrocarbon components (C1, C10, C20) = 0.1, 0.2, 0.7	Water viscosity = 1×10^{-3} Pa.s Gas injection rate = 2.208×10^{-3} m^3/s (500 barrels/d) Bottom hole pressure = 8.963 MPa (1300 psi)

The last case is a generic reservoir with 3 producer and 3 injector wells. Figure 6 shows the reservoir and hybrid mesh used. This case again refers to the gas injection into a reservoir with the same components and overall composition as case 2. Table 3 presents the fluid and physical properties for this case. The same set of relative permeability curves as shown in Fig. 5 were used for this case as well.

Table 3. Input data for Case 3.

Reservoir data	Initial conditions	Physical properties and well conditions
Reservoir area = 2.6886×10^5 m2 Reservoir thickness = 100 m (30.48 ft) Absolute permeability (K_{xx}= K_{yy} = K_{zz}) = 1.0×10^{-3} m^2 (100mD) Porosity = 0.350	Water saturation S_{wi} = 0.17 Reservoir pressure = 3.45 MPa (500 psi) Overall fraction of hydrocarbon components (C1, C10, C20) = 0.1, 0.2, 0.7	Water viscosity = 1×10^{-3} Pa.s Total Gas injected rate = 6.6204×10^{-3} m^3/s (1500 barrels/d) Bottom hole pressure = 3.45 MPa (500 psi)

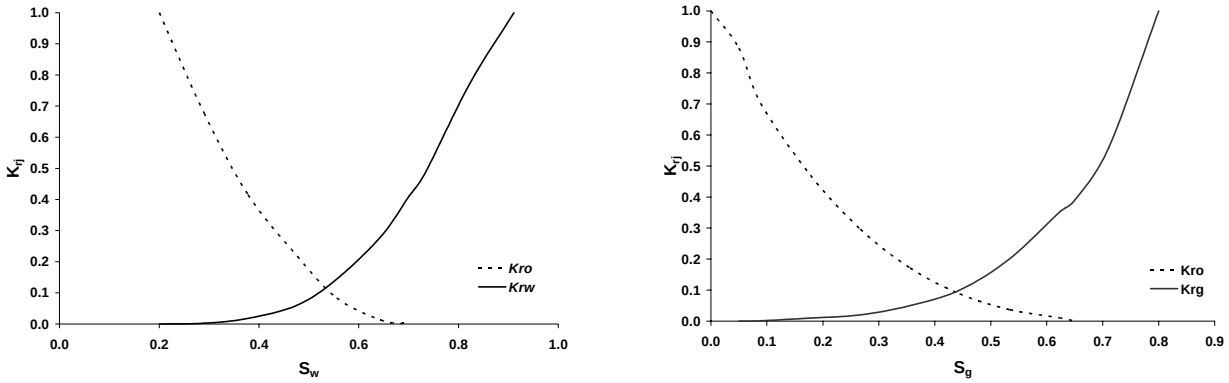

(a) (b)

Figure 5. Relative permeability curves

5. RESULTS

Figure 7 presents the results in terms of volumetric rate at standard conditions for oil, and water phases for case 1 using two-triangular meshes. It is also shown the results of this simulation using a black-oil commercial simulator. From Figure 7, it is possible to infer that the results of this work present the same trend as the ones obtained through the use of the commercial simulator. Figure 7 also shows that a close match for the results was obtained as the mesh refinements were carried out. However, some differences between this implementation and the results obtained using the commercial simulator were observed. These differences may be caused by the following effects: different equations used to obtain the physical properties such as molar densities or different transmissibilities used by the simulators. The commercial simulator used in this investigation employs inaccurate calculation of transmissibilities, as discussed in the previous section of our work, and uses elements with angles larger than a right angle. According to the literature, the usage of such angles must be avoided in CVFEM, in order to not create negative transmissibilities.

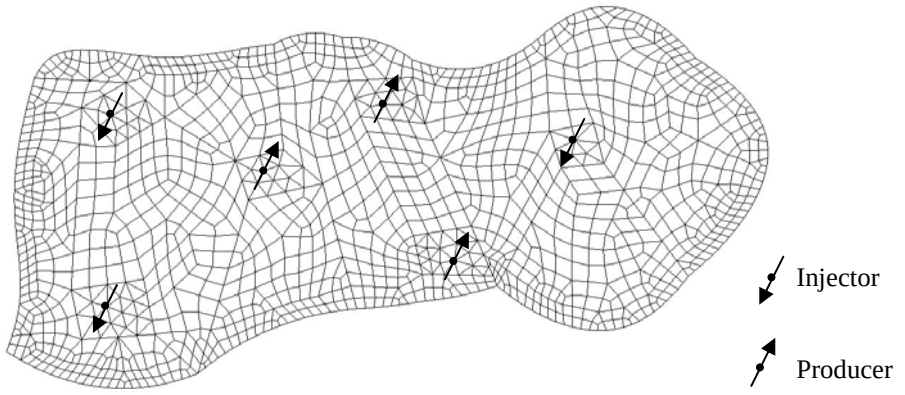

Figure 6. A 1300 elements and 1400 nodes hybrid mesh for case 3

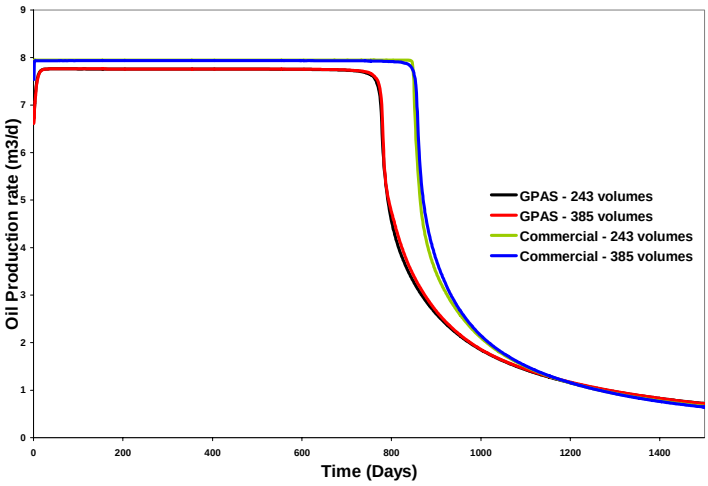

(a)

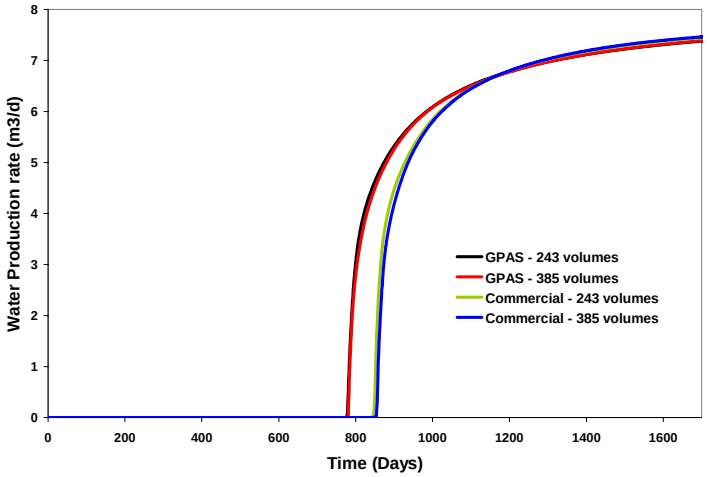

(b)

Figure 7. Results for Case 1 (a) Oil production rate vs. time (b) Water production rate vs. time

Figure 8 presents the results for case 2, for the oil and gas volumetric rates, using three different meshes: triangular, quadrilateral, and hybrid (combined triangular and quadrilateral) elements. From this figure, it can be observed that a very good agreement was obtained using different meshes, although the size of the elements and the number of vertices changed a lot for all employed meshes. Although the number of vertices for the quadrilateral mesh are higher than the ones for the triangular meshes, the triangular elements are smaller than the quadrilateral elements, therefore the quadrilateral mesh displays some differences in the results when compared to the triangular and hybrid meshes. Figures 9a and 9b present the gas front at 150 and 500 days, respectively, using the hybrid mesh. From Figure 9, it can be inferred that a radial, symmetrical sharp front is obtained, even though the hybrid-mesh employed is not very refined.

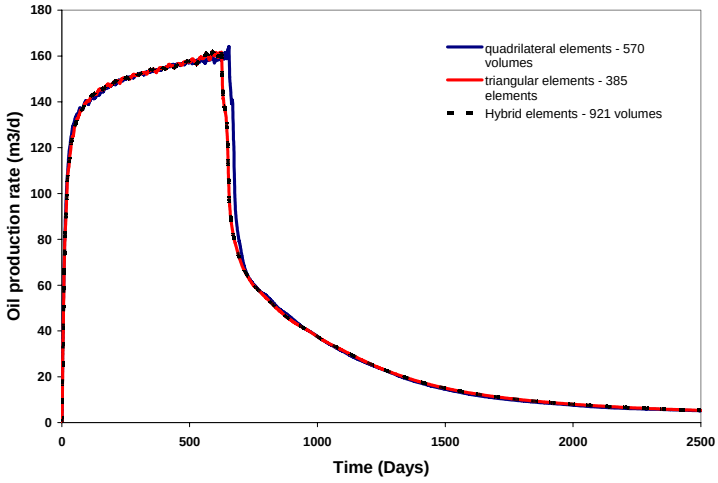

(a)

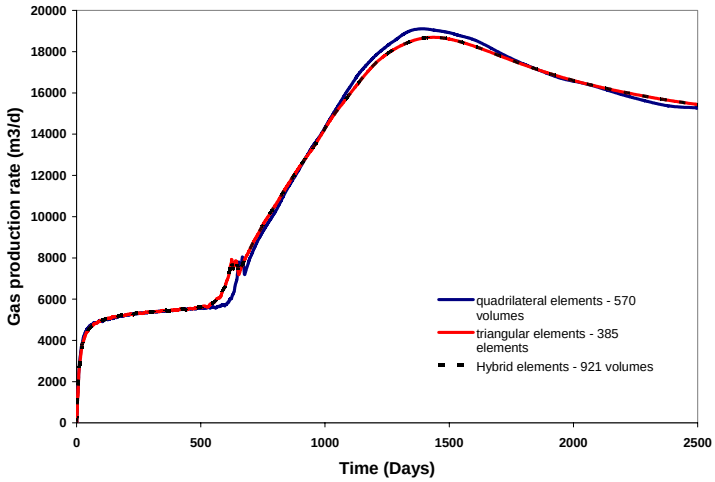

(b)

Figure 8. Results for Case 2 (a) Oil production rate vs. time (b) Gas production rate vs. time

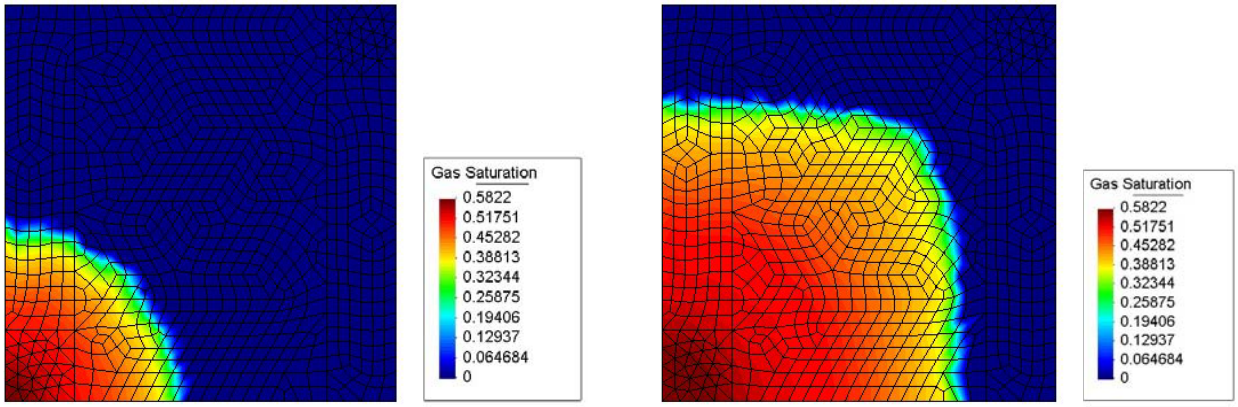

(a) (b)

Figure 9. Case 2 - Gas saturation field (a) – 150 days (b) – 500 days

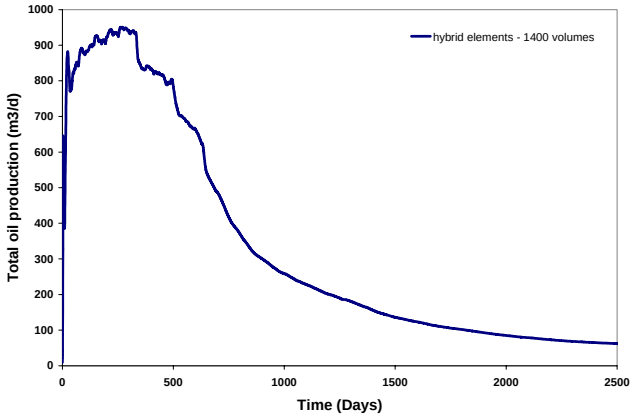

(a)

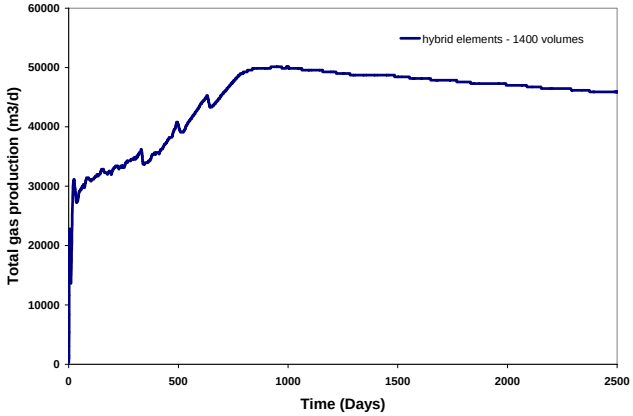

(b)

Figure 10. Results for Case 3 (a) Oil production rate vs. time (b) Gas production rate vs. time

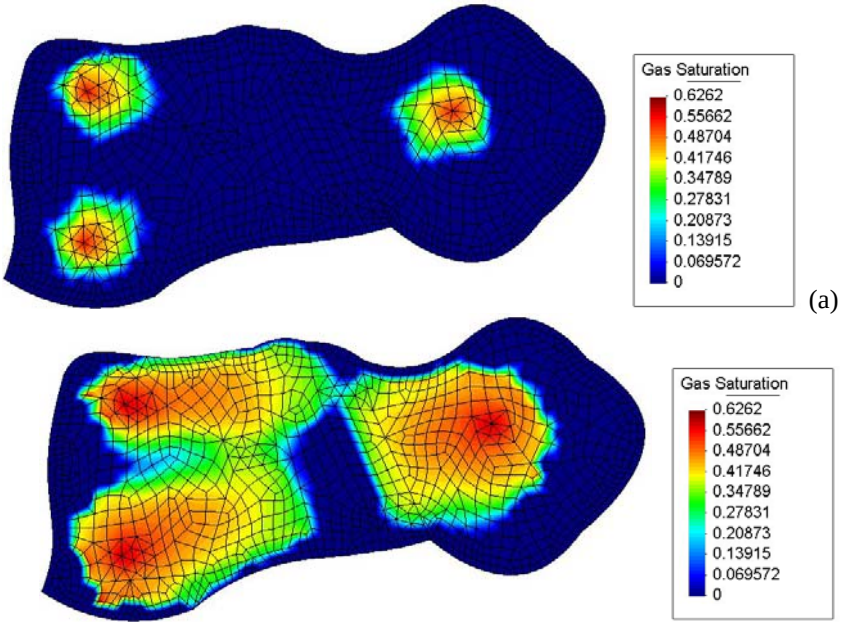

(a)

(b)

Figure 9. Case 2 - Gas saturation field (a) – 160 days (b) – 800 days

Figure 10 shows the oil and gas volumetric rates for case 3. For this case, only the mesh presented in Fig. 6 was employed. The gas front at 160 and 800 days is presented in Fig. 11. Again, sharp radial fronts, close to the injection wells are obtained, although a refined mesh was not used for this run.

6. CONCLUSIONS

An element-based finite volume approach for compositional reservoir simulation, using unstructured grids based on triangular, quadrangular and hybrid elements was presented. The results for the water flooding simulation using triangular elements were compared to the results obtained using a commercial simulator that employs a similar approach to the one developed in this work. Some differences were observed when the results of this formulation were compared with the commercial simulator. However, similar trends were observed for the results obtained using both approaches. The observed differences can be justified, based on the way the equations for the CVFEM method were obtained in our approach. The approximation equations for this formulation are obtained first for single phase flow, then, the resulting equations are multiplied by phase mobilities and molar densities rendering the equations for multiphase flow. Also, the CVFEM employed by the commercial simulator has a restriction that was not followed for the meshes employed in this comparison study. The angle of the elements used in the simulations must be equal or smaller than the right angle for the commercial simulator in order to obtain accurate results. For the gas flooding simulations, good agreements for the results were obtained using different types of elements.

7. ACKNOWLEDGEMENTS

This work was conducted with the support of the Reservoir Simulation Joint Industry Project, a consortium of operating and service companies at the Center for Petroleum and Geosystems Engineering at The University of Texas at Austin. Also, the first author would like to thank CAPES (Brazilian Educational Agency) and CNPq (The National Council for Scientific and Technological Development) for their financial support.

8. REFERENCES

Baliga, B. R. and Patankar, S. V., 1983, “A Control Volume Finite-Element Method for Two-Dimensional Fluid Flow and Heat Transfer”, Numerical Heat Transfer, vol. 6, pp. 245-261.

Cordazzo, J., 2004, “An Element Based Conservative Scheme using Unstructured Grids for Reservoir Simulation”, SPE Annual Technical Conference and Exhibition, Houston, Texas.

Cordazzo, J., Maliska, C. R., Silva, A. F. C., and Hurtado, F. S. V., 2004, “The Negative Transmissibility Issue When Using CVFEM in Petroleum Reservoir Simulation - 1. Theory”, Proceedings of the 10º Brazilian Congress of Thermal Sciences and Engineering - ENCIT 2004, Braz. Soc. of Mechanical Sciences and Engineering - ABCM, Rio de Janeiro, Brazil, Nov. 29-Dec. 03.

Cordazzo, J., Maliska, C. R., Silva, A. F. C., and Hurtado, F. S. V., 2004, “The Negative Transmissibility Issue When Using CVFEM in Petroleum Reservoir Simulation - 2. Results”, Proceedings of the 10º Brazilian Congress of Thermal Sciences and Engineering - ENCIT 2004, Braz. Soc. of Mechanical Sciences and Engineering - ABCM, Rio de Janeiro, Brazil, Nov. 29-Dec. 03.

Forsyth, P .A. 1990, “A Control-Volume, Finite-Element Method for Local Mesh Refinement in Thermal Reservoir Simulation”, SPE paper 18415, (Nov.): 561-566.

Fung, L. S., Hiebert, A. D. and Nghiem, L., 1991, “Reservoir Simulation with a Control-Volume Finite-Element Method”, SPE paper 21224 presented at the 11th SPE Symposium on Reservoir Simulation, Anaheim, California, February 17-20.

Gottardi, G. and Dall´Olio, D., 1992, “A Control-Volume Finite-Element Model for Simulating Oil-Water Reservoirs”, Journal of Petroleum Science and Engineering, 8, 29-41, Elsevier Science Publishers B. V., Amsterdam.

Hughes, T. J. R., 1987, The Finite Element Method, Linear Static and Dynamic Finite Element Analysis, Prentice Hall, New Jersey.

Maliska, C. R., 2004, “Heat Transfer and Computational Fluid Mechanics”, Florianópolis, 2ª. Ed., Editora LTC. (In Portuguese).

Parashar, M., Wheeler, J. A., Pope, G., Wang, K., and Wang, P., 1997, “A New Generation EOS Compositional Reservoir Simulator: Part II – Framework and Multiprocessing”, paper SPE 37977, SPE Reservoir Simulation Symposium, Dallas, USA.

Raw, M., 1985, “A New Control Volume Based Finite Element Procedure for the Numerical Solution of the Fluid Flow and Scalar Transport Equations”, Ph.D. Thesis, University of Waterloo, Waterloo, Ontario, Canada.

Verma, S. and Aziz, K., 1997, “A Control Volume Scheme for Flexible Grids in Reservoir Simulation”, paper SPE 37999 presented at the Reservoir Symposium, Dallas, Texas, 8-11.

Wang, P., Yotov, I., Wheeler, M., Arbogast, T., Dawson, C., Parashar, M., and Sepehrnoori, K., 1997, “A New Generation EOS Compositional Reservoir Simulator: Part I – Formulation and Discretization”, paper SPE 37079, SPE Reservoir Simulation Symposium, Dallas, Texas.

9. RESPONSIBILITY NOTICE